

Supporting Information for “Outsized contribution of the semi-arid ecosystems to interannual variability in North American ecosystems”

B. Byrne¹, J. Liu², A. A. Bloom², K. W. Bowman², Z. Butterfield³,

J. Joiner⁴, T. F. Keenan^{5,6}, G. Keppel-Aleks³, N. C. Parazoo², and Y. Yin⁷

¹NASA Postdoctoral Program Fellow, Jet Propulsion Laboratory, California Institute of Technology, CA, USA

²Jet Propulsion Laboratory, California Institute of Technology, CA, USA

³Department of Climate and Space Sciences and Engineering, University of Michigan, Ann Arbor, MI, USA

⁴Goddard Space Flight Center, Greenbelt, MD 20771, USA

⁵Earth and Environmental Sciences Area, Lawrence Berkeley National Laboratory, Berkeley, California, USA

⁶Department of Environmental Science, Policy and Management, University of California, Berkeley, Berkeley, California, USA

⁷Division of Geological and Planetary Sciences, California Institute of Technology, Pasadena, CA, USA

Contents of this file

1. Figures S1 to S9
2. Table S1

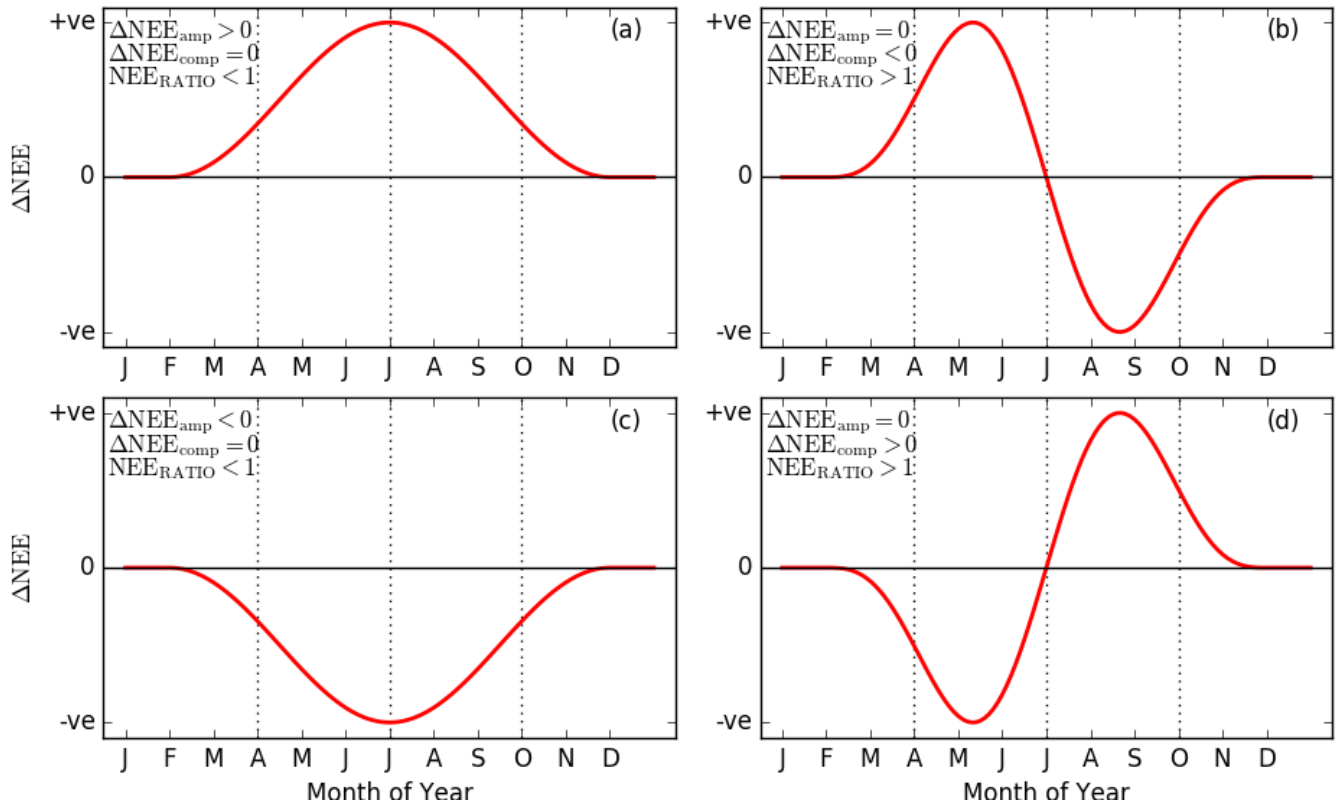


Figure S1. Illustration of amplification and compensation for NEE. (a) Positive amplification with no compensation, (b) no amplification with negative compensation, (c) negative amplification with no compensation, and (d) no amplification with positive amplification.

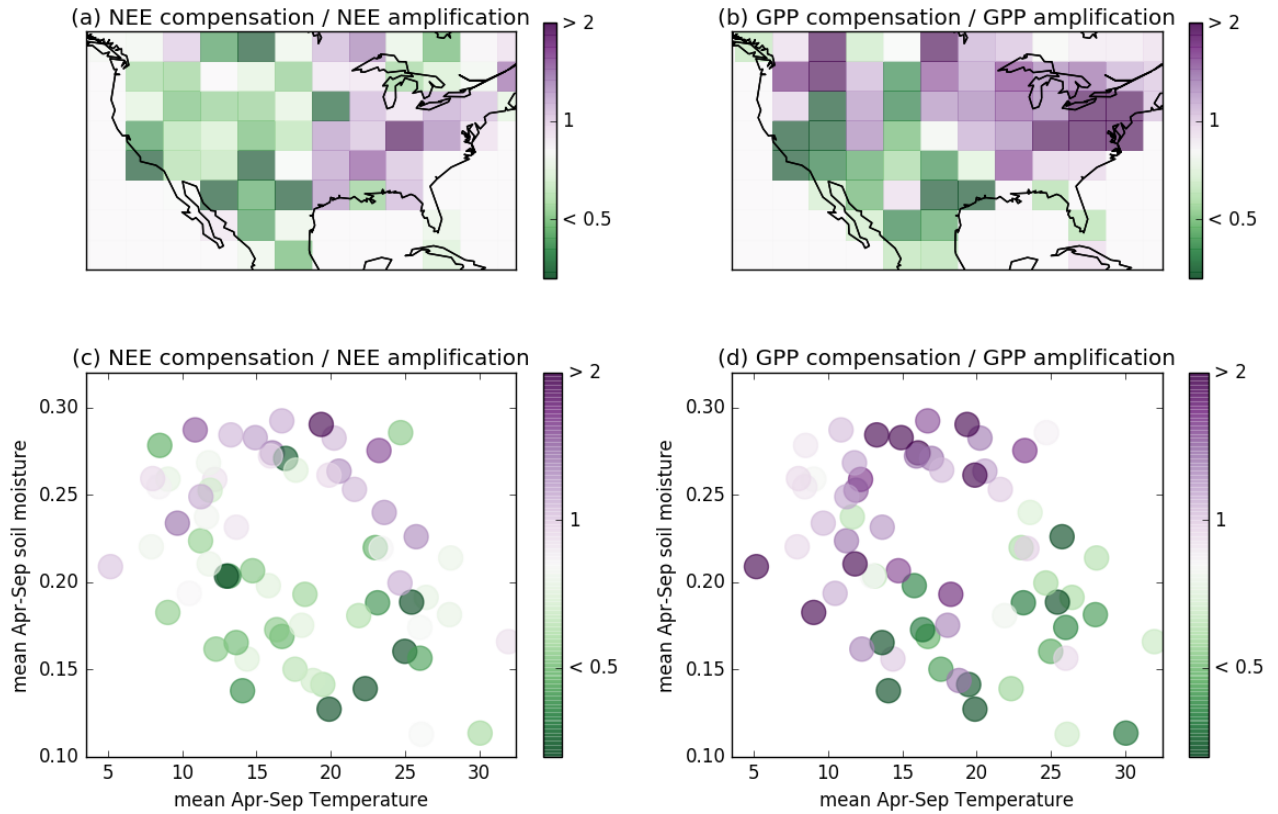


Figure S2. Relative magnitudes of seasonal compensation and amplification. (a) NEE_{RATIO} and (b) GPP_{RATIO} over 2010–2015 at $4^\circ \times 5^\circ$. (c) NEE_{RATIO} and (d) GPP_{RATIO} plotted as a function of Apr-Sep mean soil temperature and soil moisture.

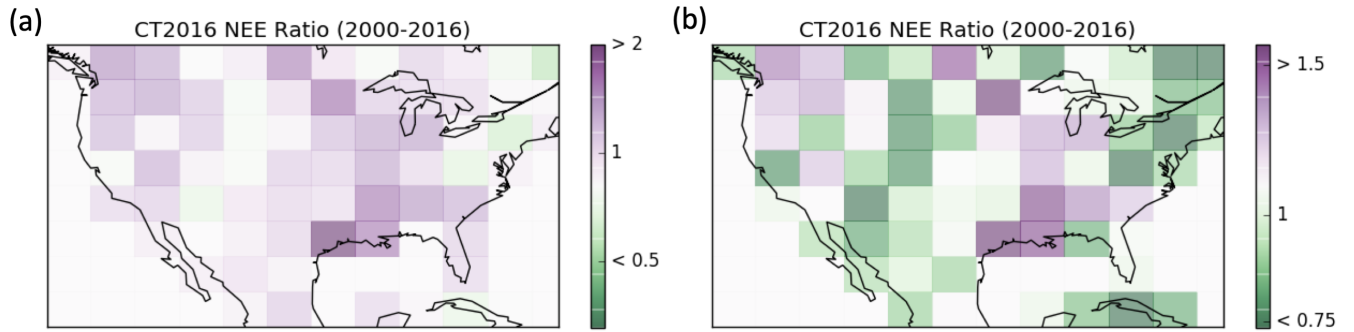


Figure S3. NEE_{RATIO} for CarbonTracker (CT2017) over 2000–2016 at $4^\circ \times 5^\circ$ spatial resolution. (a) shows with the same colorbar axis limits as Fig. 1 and (b) shows with a shifted colorbar to highlight east–west differences.

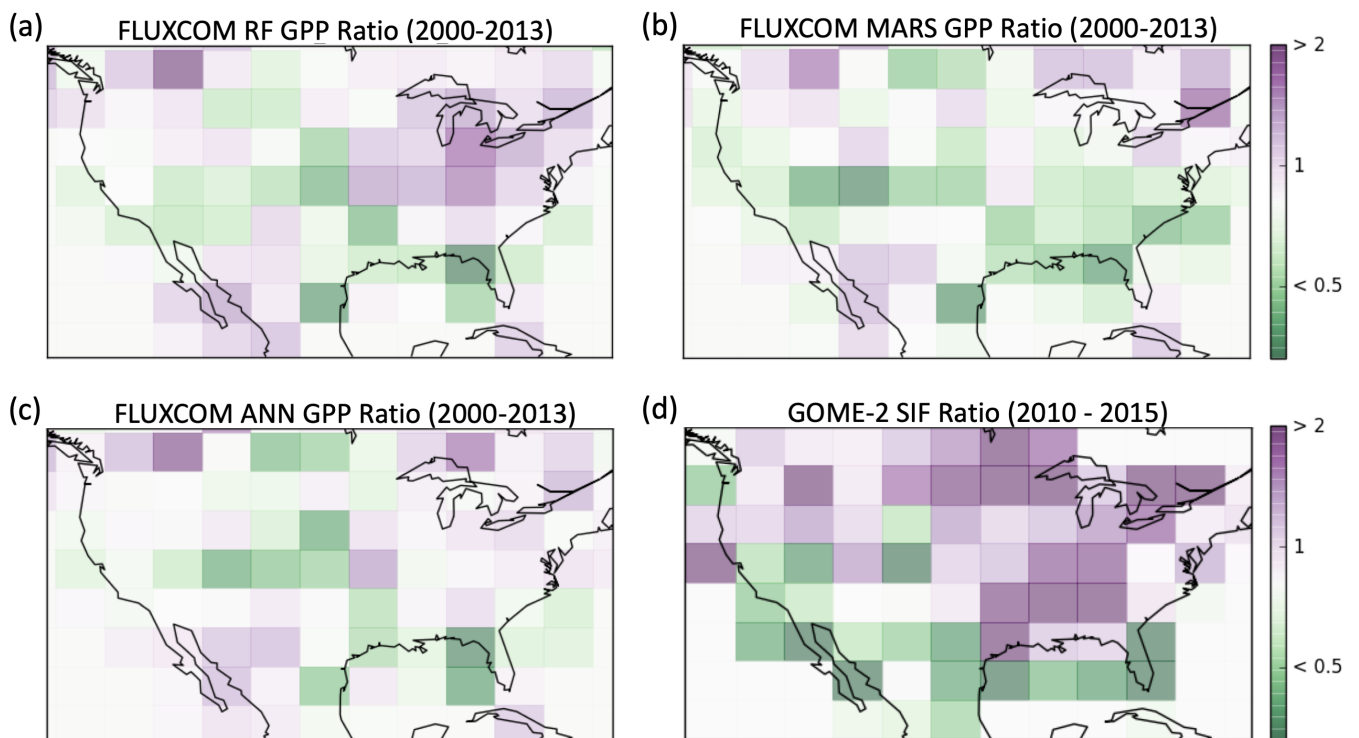


Figure S4. GPP_{RATIO} over 2000–2013 for (a) FLUXCOM RF, (b) FLUXCOM MARS, (c) FLUXCOM ANN, and (d) SIF_{RATIO} over 2010–2015 for GOME-2 SIF.

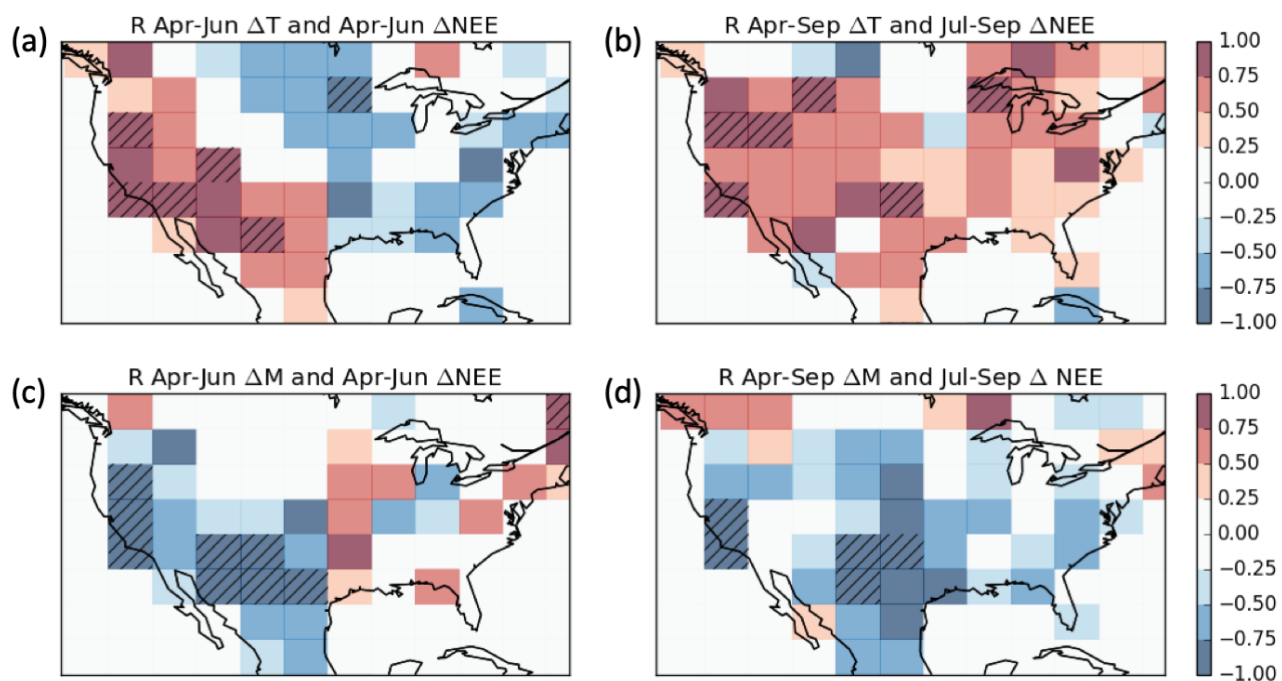


Figure S5. Relationship between ΔNEE and variations in climate. Coefficient of correlation (R) over 2010–2015 for $4^\circ \times 5^\circ$ grid cells between (a) Apr–Jun ΔT and Apr–Jun ΔNEE , (b) Apr–Sep ΔT and Jul–Sep ΔNEE , (c) Apr–Jun ΔM and Apr–Jun ΔNEE and (d) Apr–Sep ΔM and Jul–Sep ΔNEE . Hatching shows grid cells for which $P < 0.05$.

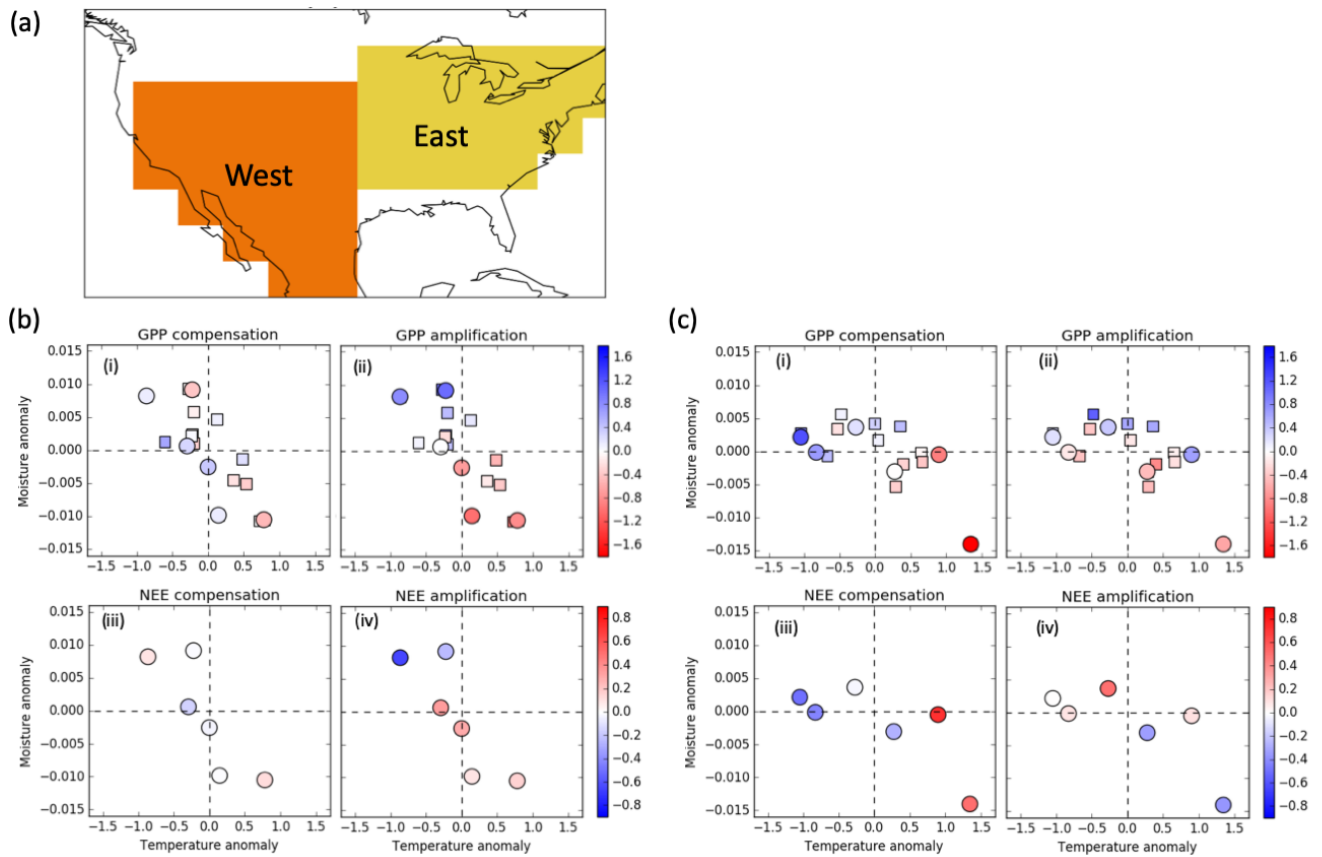


Figure S6. Regional seasonal compensation and amplification components as a function of ΔT and ΔM . (a) Spatial extent of western (orange) and eastern (yellow) regions of North America. (b) Western and (c) Eastern scatter plots of (i) ΔGPP_{comp} , (ii) ΔGPP_{amp} , (iii) ΔNEE_{comp} and (iv) ΔNEE_{amp} as a functions of ΔT and ΔM . NEE covers the period 2010–2015 and GPP covers the period 2001–2017, with circles indicating points over 2010–2015 and squares indicating points outside this time period.

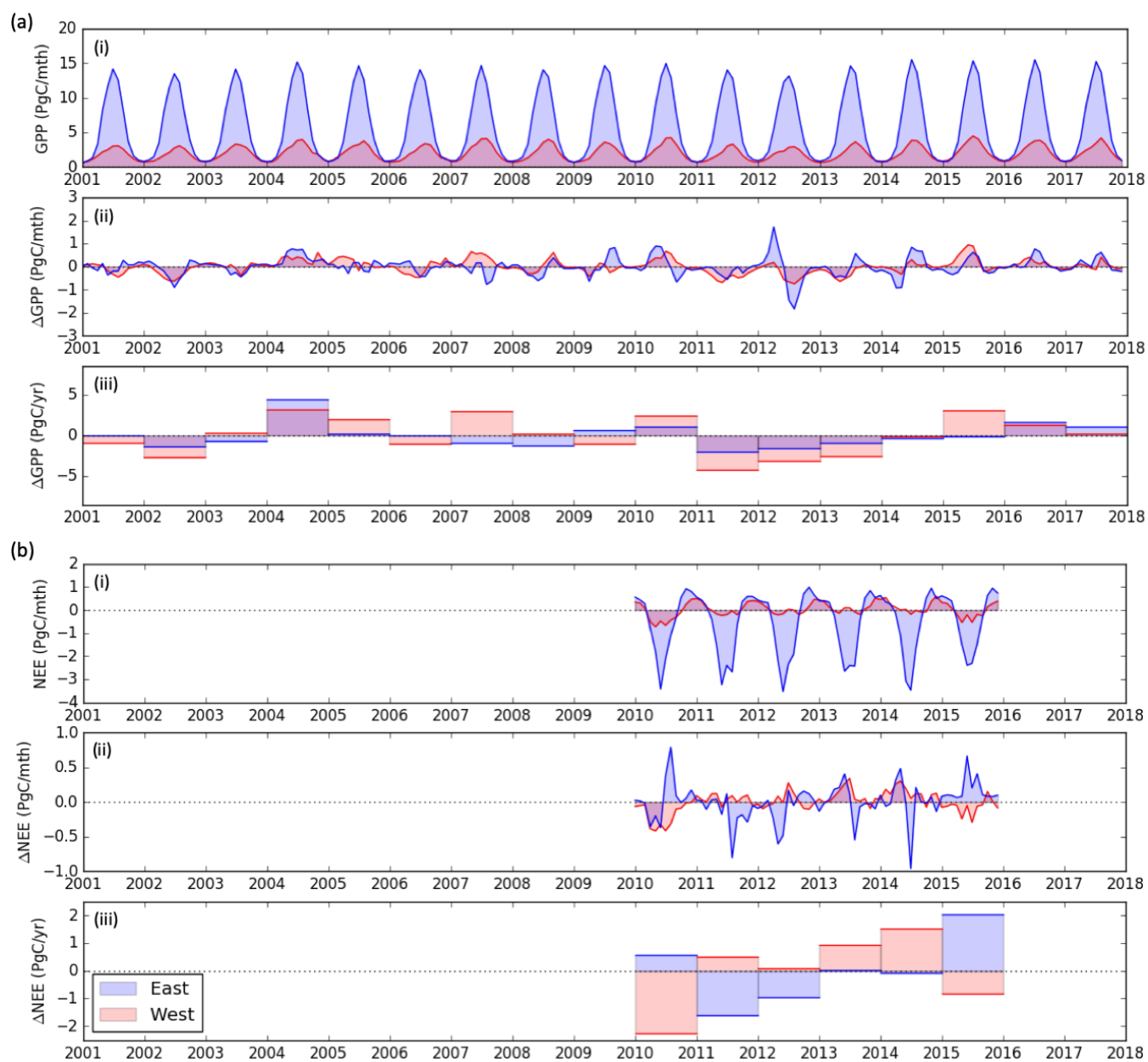


Figure S7. Timeseries of (a) GPP (2001–2017) and (b) NEE (2010–2015) in western (shaded red area) and eastern (shaded blue area) North America. For GPP and NEE, panel (i) shows the seasonal cycle, (ii) shows the monthly anomalies, and (iii) shows the yearly anomalies.

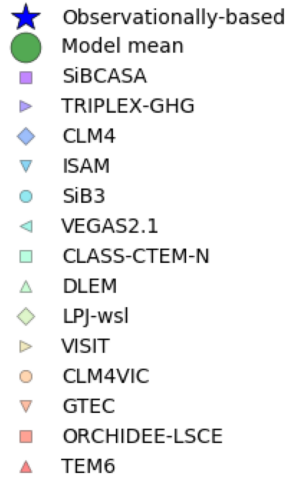


Figure S8. Legend of symbols plotted in Fig. 5 of the main text.

Table S1. Correlation coefficient (R) between CO₂ flux anomalies and $\Delta T_{\text{Apr-Sep}}$, $\Delta M_{\text{Apr-Sep}}$, $\Delta P_{\text{Apr-Sep}}$, or $\Delta \text{TWS}_{\text{Apr-Sep}}$. Correlations cover the period 2001–2017 for ΔGPP and 2010–2015 for ΔNEE , except for correlations with ΔTWS which cover 2003–2014 and 2010–2014. For eastern North America, 2012 is excluded for ΔGPP correlations because it is an extreme event and has a large impact on the correlation.

Region	Environ Var	$\Delta \text{GPP}_{\text{amp}}$	$\Delta \text{GPP}_{\text{comp}}$	$\Delta \text{NEE}_{\text{amp}}$	$\Delta \text{NEE}_{\text{comp}}$
West	$\Delta T_{\text{Apr-Sep}}$	-0.71	-0.41	0.63	0.22
West	$\Delta M_{\text{Apr-Sep}}$	0.91	0.09	-0.66	-0.13
West	$\Delta P_{\text{Apr-Sep}}$	0.78	0.31	-0.47	-0.21
West	$\Delta \text{TWS}_{\text{Apr-Sep}}$	0.50	0.20	-0.70	-0.19
East	$\Delta T_{\text{Apr-Sep}}$	-0.09	-0.81	-0.46	0.89
East	$\Delta M_{\text{Apr-Sep}}$	0.72	0.41	0.78	-0.49
East	$\Delta P_{\text{Apr-Sep}}$	0.35	0.31	0.48	-0.44
East	$\Delta \text{TWS}_{\text{Apr-Sep}}$	0.56	0.31	0.81	-0.30

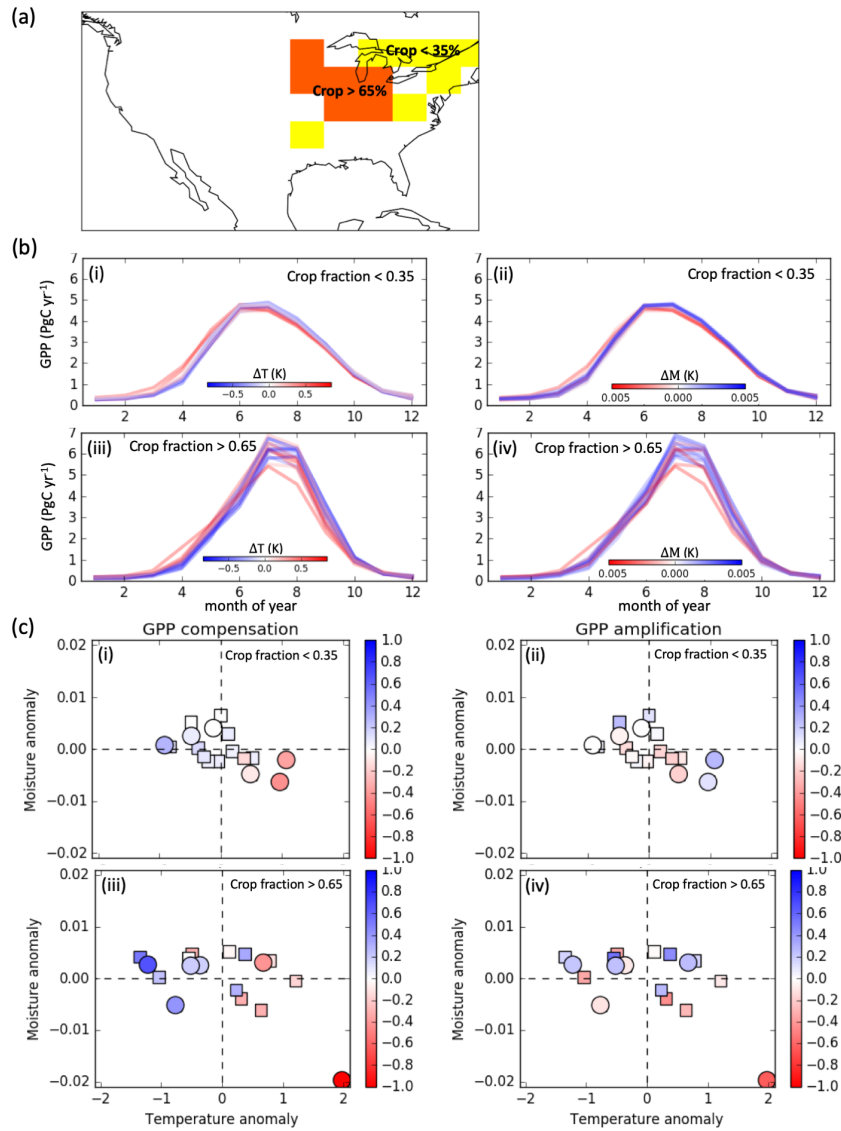


Figure S9. (a) Grid cells with crop fractions $> 65\%$ or $< 35\%$. (b) Time series of 2001-2017 GPP as a function of month of year for grid cells with crop fractions $< 35\%$ ((i) and (ii)) and crop fractions $> 65\%$ ((iii) and (iv)). Curves are colored by Apr-Sep temperature anomaly for (i) and (iii), and are colored by Apr-Sep moisture anomaly for (ii) and (iv). (c) Seasonal compensation ((i) and (iii)) and amplification ((ii) and (iv)) components for grid cells with crop fractions $< 35\%$ and $> 65\%$. Note that the outlier for crop fractions $> 65\%$ is due to the 2012 North American Drought.